Exploring the Surface Reactivity of Ag Nanoparticles with Antimicrobial Activity: A DFT Study

Rubén E. Estrada-Salas,[a] Hector Barrón,[a] Ariel A. Valladares,*[b] and Miguel José-Yacamán[a]

The preferential sites of electrophilic, nucleophilic, and radical attacks on the surface of highly spherical Ag nanoparticles with a diameter of ~ 2 nm are studied via the Fukui functions and the molecular electrostatic potential; both are calculated using the density functional (DFT) generalized gradient approximation-revised version of the Perdew, Burke, and Ernzerhof level of theory with the double-numerical with polarization functions (DNP) basis set for the valence electrons, and DFT-based semicore pseudopotentials for the core electrons. Because the interaction of Ag nanoparticles with virus and microorganisms takes place in an aqueous environment, the solvent (water) effect is also obtained using the Conductor-like Screening Model. Three typical structures are chosen: cuboctahedral, icosahedral, and ino-decahedral. All three present an "amphoteric" behavior against electrophiles, nucleophiles, and radicals. For the cuboctahedral and decahedral geometries, the highest susceptibility to attack is on the edges shared by a {111} face and a {100} face; for the icosahedral geometry, the highest susceptibility to attack is on the vertices. Ionization potentials, electron affinities, electronegativities, and chemical hardness are also reported. Comparison with experiments is presented. © 2012 Wiley Periodicals, Inc.

DOI: 10.1002/qua.24207

Introduction

Ag nanoparticles have received considerable attention due to their capacity to interact with viruses (such as HIV-1)[1,2] as well as their bactericidal, antifungal, and antimicrobial properties (Fig. 1).[3–8] In both cases, it has been found that only nanoparticles in the range of 1–10 nm interact with the virus or the bacteria.[1,3] However, there are some questions which need to be addressed, such as the exact mechanism of interaction of silver nanoparticles with the bacterial cells and how the surface area of nanoparticles influences its killing activity.[4] Therefore, it is important to get a better understanding of the dependence of the Ag nanoparticles surface reactivity with size, but first we want to understand the reactivity of a typical silver nanoparticle. To this end, we have performed density functional (DFT) calculations of the molecular electrostatic potential (MEP) and of the Fukui functions—two useful reactivity indices[9–11]—for highly spherical silver nanoparticles with a diameter of 2.08 nm. We chose this size and shape for the nanoparticle because this is the mean diameter of nearly 75% of the nanoparticles synthesized by Elechiguerra et al.,[1] which are conjugated to bovine serum albumin protein molecules. According to Diaz-Torres et al.,[2] this is a facile and rapid method for the synthesis of Ag nanoparticles.

To predict a system's reactive behavior, a number of theoretical reactivity indices, obtainable from the electron density $\rho(r)$, are available. One of them is the frequently used MEP, $\phi(r)$, defined as the interaction energy of the system studied (e.g., a molecule, a surface, or a particle) with a positive test charge placed at position r:[9,12]

$$\phi(r) = \sum_{A} \frac{Z_A}{|r - r_A|} - \int \frac{\rho(r')}{|r - r'|} dr' \quad (1)$$

where the summation runs over all the nuclei A in the system. Due to its definition, the MEP can be used in the study of electrophilic attacks and is expected to describe mainly the hard–hard interactions between the reacting systems because its mathematical definition does not contemplate variations in the electron density.[9] An electrophilic species will preferentially attack at sites where the MEP is most negative. MEPs provide insight into molecular recognition processes such as enzyme–substrate and drug–receptor interactions.[12]

The Fukui function, describing the soft–soft interactions between the reagents, whose mathematical definition does contemplate variations in the electron density, is defined as:[9,13]

$$f(r) = \left[\frac{\delta \mu}{\delta v(r)}\right]_N = \left[\frac{\partial \rho(r)}{\partial N}\right]_v \quad (2)$$

[a] *R. E. Estrada-Salas, H. Barrón, M. José-Yacamán*
Department of Physics and Astronomy, University of Texas at San Antonio, San Antonio, Texas 78249
[b] *A. A. Valladares*
Departamento de Materia Condensada y Criogenia, Instituto de Investigaciones en Materiales, Universidad Nacional Autónoma de México, México D.F., C.P. 04510, México
E-mail: valladar@unam.mx

Contract grant sponsor: CONACyT (R.E.E.S.), DGAPA-UNAM (A.A.V.).
Contract grant sponsor: Welch Foundation Project (H.B. and M.J.Y.); contract grant number: AX-1615.
Contract grant sponsor; National Science Foundation (NSF) PREM (H.B. and M.J.Y.); contract grant number: DMR 0934218.
Contract grant sponsor: NIH-RCMI Center for Interdisciplinary Health Research (H.B. and M.J.Y.); contract grant number: 2G12RR013646-11.
Contract grant sponsor: The NSF (H.B. and M.J.Y.); contract grant number: DMR-1103730.

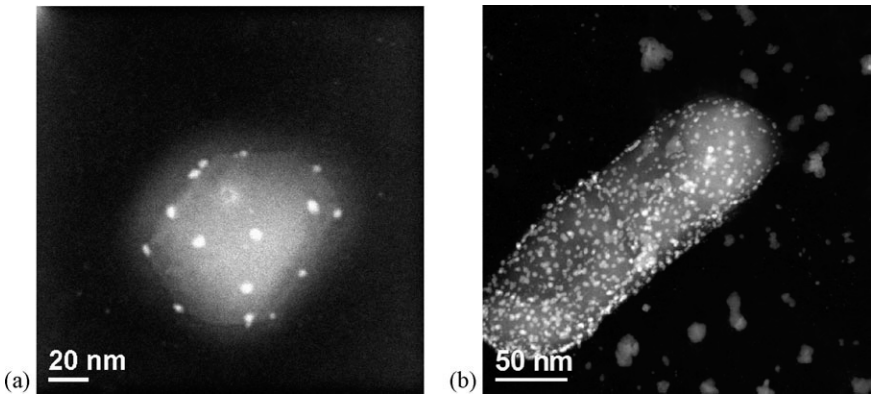

Figure 1. Electron microscopy images showing the interaction of silver nanoparticles with: a) an HIV-1 virus, and b) an *E. coli* bacteria (these electron microscopy images were taken at the Dr. M. J. Yacaman's Laboratory of Nanomaterials, Department of Physics and Astronomy, University of Texas at San Antonio).

Because of the discontinuity in Eq. (2)—the electron number N can change only by integer values—different physical meanings have been associated with the left and right derivatives as well as with their average value, corresponding to a reactivity index for an electrophilic [$f^-(r)$], a nucleophilic [$f^+(r)$], and a radical attack [$f^0(r)$], respectively.[9,13]

Other chemical properties suitable for analyzing chemical reactivity were also used, namely the ionization potential I_P, the electron affinity E_A, the electronegativity χ, and the chemical hardness η of each nanoparticle studied.

The I_P is defined as the amount of energy necessary to remove one electron from a chemical species (i.e., atom, molecule, cluster, etc.) in the gas phase:[14]

$$X^0_{(g)} \rightarrow X^+_{(g)} + e^-; \Delta E = I_p \tag{3}$$

The I_P can be calculated as the difference between the energy of the positively charged species E^+ and the energy of the neutral species E^0:

$$I_P = E^+ - E^0 \tag{4}$$

The E_A is related to the energy of the process of accepting one electron from a chemical species:[14]

$$X^0_{(g)} + e^- \rightarrow X^-_{(g)};\ \Delta E = E_A \tag{5}$$

The E_A can be calculated as the difference between the energy of the neutral species E^0 and the energy of the negatively charged species E^-:

$$E_A = E^0 - E^- \tag{6}$$

The χ is defined as the tendency of a species to attract electrons. It can be calculated as the average between the I_P and the E_A:[15]

$$\chi = \frac{I_P + E_A}{2} \tag{7}$$

Finally, the chemical hardness η is also defined in terms of the I_P and the E_A[15] by using the following equation:

$$\eta = \frac{I_P - E_A}{2} \tag{8}$$

The χ and η are usually taken as absolute values and are very useful properties in the study of the chemical reactivity of different species.[15]

Calculation details

Full geometry optimizations and total energy calculations were performed with the DFT-based program package DMol[3] at the generalized gradient approximation level of theory.[16–18] Specifically, we used the revised version of the Perdew, Burke, and Ernzerhof (RPBE) functional[19] with double numerical atomic orbital basis sets plus polarization functions (DNP)[20] for the treatment of the valence electrons and DFT-based semicore pseudopotentials (DSPPs)[21] for the treatment of the core electrons. DSPPs introduce some degree of relativistic correction into the core, such relativistic corrections are important in the study of heavy elements like silver.

We chose this level of theory because the large dimension of the systems makes the use of higher order theoretical approaches such as the second-order many-body perturbation method or the configuration interaction method, unfeasible. We decided to use the RPBE DFT because it presents essentially the same performance as the well tested PW91[22] and Perdew, Burke, and Ernzerhof (PBE)[23] functionals, but improves the calculation of adsorption energies[19] and therefore, it is more suitable in studies of surface reactivity.

Due to the fact that the interaction of Ag nanoparticles with viruses and microorganisms takes place in an aqueous environment, and the solvent (water) effect was also taken into account by using the Conductor-like Screening Model.[24,25] As it is shown in the Results and Discussion section, clear differences in the surface reactivity, with and without the effect of the solvent, were found.

Because of the face-centered-cubic (FCC) crystalline structure of silver, the atomistic models of the nanoparticles with a diameter of ~2 nm cannot be completely spherical in shape; therefore, we chose the three typical structures that have been observed for small particles of materials whose bulk structure is FCC: cuboctahedral, icosahedral, and decahedral, Figure 2. Each of these three structures consists of 147 silver atoms, the magic number corresponding to the size of ~2 nm.[26]

For a clear visualization of the silver nanoparticles surface reactivity, both the calculated MEP and Fukui functions were mapped onto an isosurface of the total electron density of each nanoparticle, showing the sites of high susceptibility to electrophilic, nucleophilic, and radical attacks on the nanoparticle surface.

The ionization potentials and the electron affinities were calculated taking the energy differences between the total

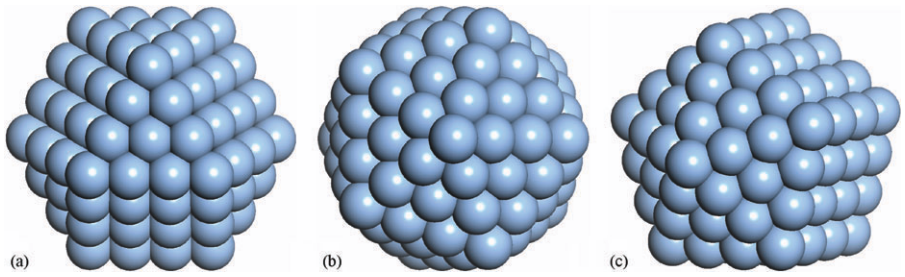

Figure 2. Atomic structures of the 2-nm silver nanoparticles studied: a) cuboctahedron, b) icosahedrons, and c) Ino-decahedron. The three nanoparticles are made of 147 Ag atoms. [Color figure can be viewed in the online issue, which is available at wileyonlinelibrary.com.]

energy of each of the positively charged, the neutral, and the negatively charged nanoparticles [using Eqs. (4) and (6)]. The electronegativities were then calculated with Eq. (7).

Results and Discussion

After the geometry optimization of the silver nanoparticles with and without the solvent effect, we could see that both their geometry and symmetry remained practically unchanged, except for a small increase of 0.05 Å in the Ag-Ag interatomic distance. The minimal energy structure corresponds to the icosahedral nanoparticle; however, its total energy is only 5 eV lower than the cuboctahedral nanoparticle and 3.5 eV lower than the ino-decahedral one. The total energy of each nanoparticle is: cuboctahedral: −739,563.17 eV, icosahedral: −739,568.33 eV, and ino-decahedral: −739,565.08 eV; therefore, it can be assumed that the three different geometries have almost the same stability for this size range.

Figures 3–5 show a comparative visualization of the preferential reactive sites on the surfaces of the Ag nanoparticles against electrophilic, nucleophilic, and radical attacks. We can observe that the three different geometries present an "amphoteric" behavior against electrophiles, nucleophiles, and radicals. If we analyze the Fukui functions that take into account the solvent effect, we can see that for the cuboctahedral and decahedral geometries the highest susceptibility to an attack is on the edges shared by the {111} and the {100} faces, Figures 2 and 4; whereas for the icosahedral geometry, the highest susceptibility to an attack is on the vertices, Figure 3. On the other hand, analyzing the Fukui functions that do not take into account the solvent effect, we can see that the highest susceptibility to an attack is on the vertices, for the three geometries considered. Some comparisons with experimental studies are made below.

In the case of the MEP (Figs. 3g,h–5g,h), we can see that both MEPs, with and without the solvent effect, show practically the same behavior as the Fukui functions that do not take into account the solvent effect; that is, the preferential reactive sites for the three geometries considered are the vertices, according to the MEPs. Remembering that the MEP is more suitable for studying hard–hard interactions—due to the fact that its mathematical definition does not contemplate deformations in the electron density—we can deduce that the nanoparticles studied will be chemically harder in the gas phase (without the solvent effect) than in solution with water. Besides, these results also show that the icosahedral nanoparticle is harder (chemically speaking) than its cuboctahedral and decahedral counterparts whether in solution or in the gas phase.

The results mentioned earlier can be corroborated with the direct calculation of the chemical hardness of the nanoparticles studied. As seen in Table 1, the three geometries considered present a higher chemical hardness in the gas phase (without the solvent effect) than in water solution. Again, the

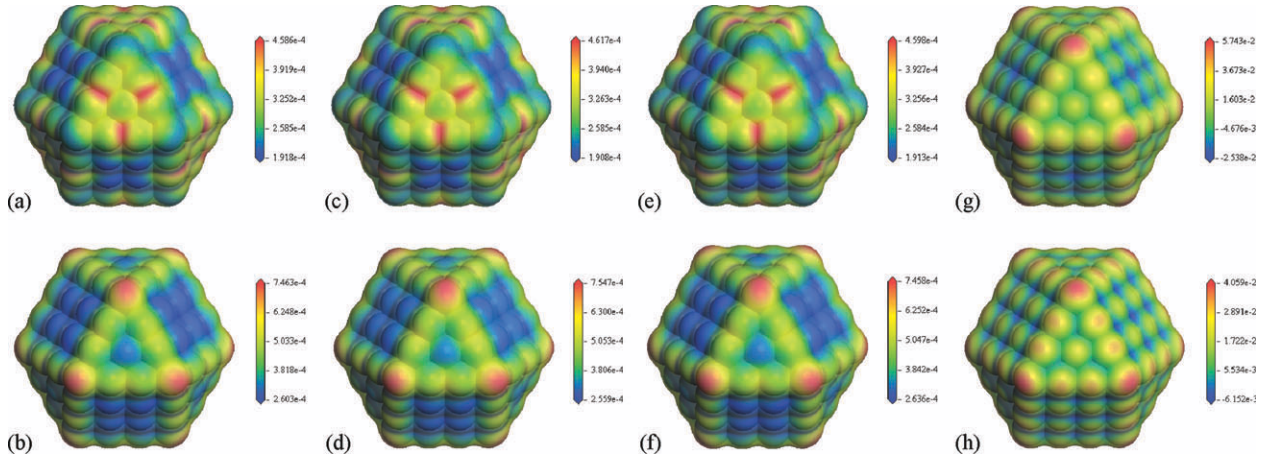

Figure 3. Electrophilic Fukui functions a) with and b) without the solvent effect (water); nucleophilic Fukui functions c) with and d) without the solvent effect; radical Fukui function e) with and f) without the solvent effect, and MEP g) with and h) without the solvent effect mapped onto an isosurface of the total electron density (isovalue = 0.017 a.u.) for the 2-nm cuboctahedral Ag nanoparticle. For the Fukui functions, red zones show the highest susceptibility to an attack, whereas blue zones show the lowest one. For the MEP, red zones show its most positive value, whereas blue zones show its most negative one. An electrophilic species will preferentially attack at sites where the MEP is most negative[7]. [Color figure can be viewed in the online issue, which is available at wileyonlinelibrary.com.]

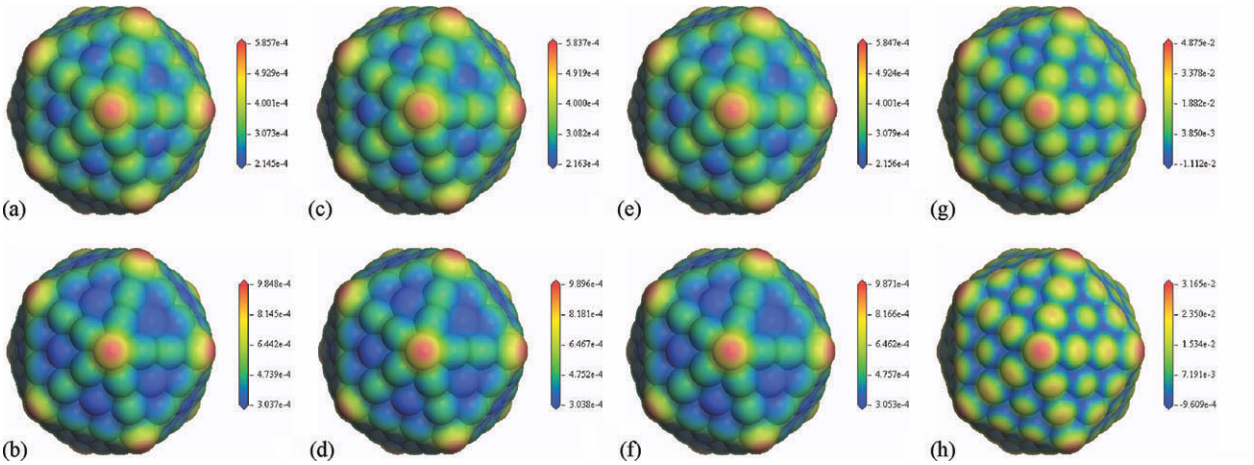

Figure 4. Electrophilic Fukui functions a) with and b) without the solvent effect (water); nucleophilic Fukui functions c) with and d) without the solvent effect; radical Fukui function e) with and f) without the solvent effect, and MEP g) with and h) without the solvent effect mapped onto an isosurface of the total electron density (isovalue = 0.017 a.u.) for the 2-nm icosahedral Ag nanoparticle. For the Fukui functions, red zones show the highest susceptibility to an attack, whereas blue zones show the lowest one. For the MEP, red zones show its most positive value, whereas blue zones show its most negative one. An electrophilic species will preferentially attack at sites where the MEP is most negative[7]. [Color figure can be viewed in the online issue, which is available at wileyonlinelibrary.com.]

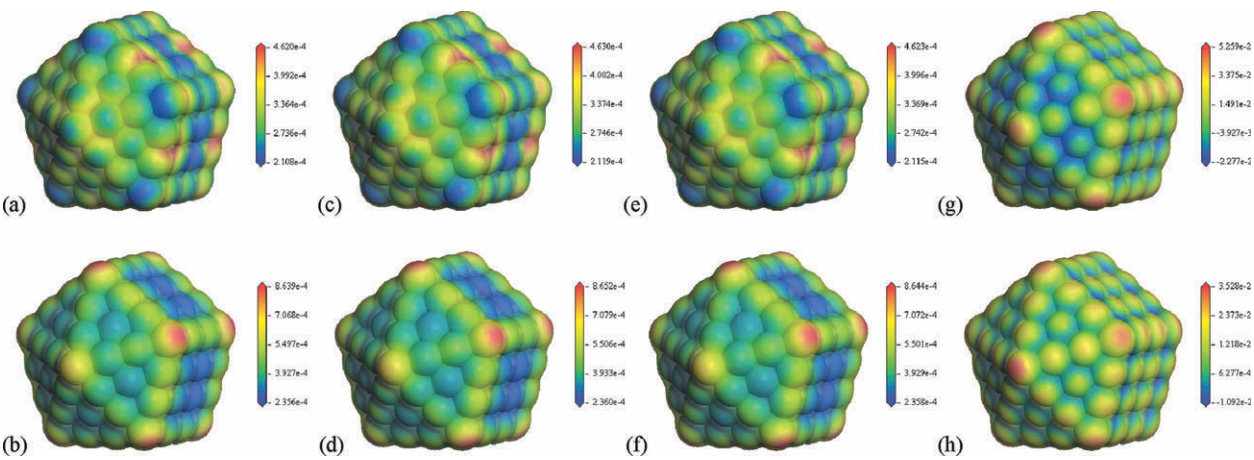

Figure 5. Electrophilic Fukui functions a) with and b) without the solvent effect (water); nucleophilic Fukui functions c) with and d) without the solvent effect; radical Fukui function e) with and f) without the solvent effect, and MEP g) with and h) without the solvent effect mapped onto an isosurface of the total electron density (isovalue = 0.017 a.u.) for the 2-nm Ino-decahedral Ag nanoparticle. For the Fukui functions, red zones show the highest susceptibility to an attack, whereas blue zones show the lowest one. For the MEP, red zones show its most positive value, whereas blue zones show its most negative one. An electrophilic species will preferentially attack at sites where the MEP is most negative[7]. [Color figure can be viewed in the online issue, which is available at wileyonlinelibrary.com.]

Table 1. Ionization potentials, electron affinities, electronegativities, chemical hardness, and HOMO–LUMO gaps of the nanoparticles studied.

	Ionization potential (I_P) [eV]		Electron affinity (E_A) [eV]		Electronegativity (χ) [eV]		Chemical hardness (η) [eV]		HOMO–LUMO gap (Eg) [eV]	
Species	With solvent effect	Without solvent effect	With solvent effect	Without solvent effect	With solvent effect	Without solvent effect	With solvent effect	Without solvent effect	With solvent effect	Without solvent effect
Cuboctahedral nanoparticle	2.928	4.358	2.892	2.786	2.910	3.572	0.018	0.786	0.068	0.058
Icosahedral nanoparticle	2.911	4.368	2.854	2.756	2.883	3.562	0.029	0.806	0.162	0.206
Ino-decahedral nanoparticle	2.887	4.296	2.849	2.724	2.868	3.510	0.019	0.786	0.101	0.094
Ag^+	7.889	5.456	2.952	7.748	5.421	6.602	2.469	1.146	3.712	4.690

A comparison with the properties of a silver cation (Ag^+) is shown.

icosahedral nanoparticle presents the highest hardness in both cases, whether or not we include the solvent effect.

The calculated values for the highest occupied molecular orbital (HOMO)–lowest unoccupied molecular orbital (LUMO) gaps of each of the studied nanoparticles also support these findings (Table 1). It is well known that hard molecules have a large HOMO–LUMO gap, and soft molecules have a small HOMO–LUMO gap;[15] therefore, the lower values obtained for the HOMO–LUMO gaps when taking into account the solvent effect indicate that the nanoparticles are harder in the gas phase than in water solution. Once again, the icosahedral nanoparticle is the hardest of the three nanoparticles studied since it presents the highest value for the HOMO–LUMO gap.

Morones et al.[3] and Pal et al.[8] proposed that the {111} faces of the Ag nanoparticles are the most reactive sites on the nanoparticle surfaces. Our results show that—at least for the nanoparticle size studied (i.e., ~2 nm)—the more reactive sites are not precisely located on top of the {111} faces but on the edges shared by a {111} and a {100} face (in the case of the cuboctahedral and decahedral nanoparticles) as well as on the vertices (in the case of the icosahedral nanoparticle). It is evident, however, that the atoms of these edges and vertices are also part of the {111} faces; therefore, in some sense we can say that parts of the {111} faces are the most reactive sites for the nanoparticles studied. Nevertheless, as the size range studied by Morones et al.[3] and Pal et al.[8] includes nanoparticles from 1 to 100 nm, it can be expected that the most reactive sites on the surfaces of the nanoparticles will change with size; therefore, as the nanoparticle increases in size, the most reactive sites might become localized on top of the {111} faces. Further theoretical studies regarding the size dependence of the reactivity of Ag nanoparticles are encouraged.

It has been long proposed that the antimicrobial mechanism of silver nanoparticles is mainly due to the release of silver ions (Ag^+) from the nanoparticle surface; however, experimental results by Despax et al.[5] indicated that Ag^+ ions released from nanosilver structures did not constitute the main (or the sole) vector of interaction with sulfur (S) or phosphorus (P) containing compounds, that is, proteins, nucleic acids, and so forth. They also found the formation of Ag/S clusters inside the cells when treating the microorganisms with silver ions (Ag^+), and the formation of Ag/S/P clusters when treating the microorganisms with nanosilver, indicating clear differences in the reactivity of Ag^+ and silver nanostructures.

To get insight on the differences in the reactivity of these two distinct silver species—Ag^+ and nanosilver—we also performed calculations of the reactivity of a single silver ion (Ag^+) for comparison with the silver nanoparticles studied (see Table 1). The fact that the silver ions form only Ag/S clusters inside the cells, whereas the nanosilver treatment leads to the formation of Ag/S/P clusters[5] can be correlated with the notably distinct electronegativity, chemical hardness, and HOMO–LUMO gap shown by each species. As is evident from Table 1, a single Ag^+ ion is considerably more electronegative and harder than any of the three Ag nanoparticles studied (cubo-, ico-, and decahedral). This indicates that Ag^+ prefers to interact with sulfur as it is more electronegative and harder than phosphorus, which can explain in part why some experiments[5] found that silver ions only form Ag/S clusters without any significant amount of phosphorus inside the cells. On the other hand, the presence of Ag/S/P clusters found inside the microorganisms when treating them with nanosilver[5] can be explained by the presence of two different silver species, namely the Ag nanoparticles—which possibly will prefer to interact with the softer phosphorus atoms rather than with the harder sulfur ones—and the Ag^+ ions released by the silver nanoparticles.

Some recent works assume that the biocide activity of silver nanoparticles is due to their radical character.[3,5,6] This is in agreement with our work as the "amphoteric" behavior against electrophiles and nucleophiles shown by the calculated Fukui functions of the Ag nanoparticles studied is a typical behavior of any radical species.

It has long been pointed out that the antimicrobial activity of silver nanoparticles is critically dependent on particle size, shape, and surface oxidation.[5–8] For example, Lok et al.[7] have indicated that partially surface-oxidized nanosilver (~9 nm) exhibits antibacterial activities, whereas zero-valent nanosilver does not. They also indicated that the smaller silver nanoparticles had higher antibacterial activity than the bigger ones. Although our calculations cannot give insight into the surface oxidation dependence of the nanoparticles reactivity, they do shed light on some other issues, mainly on those concerning the shape dependence as well as the solvent dependence of the Ag nanoparticles reactivity.

Summary and Conclusions

Our calculations indicate that, for the nanoparticle size studied (~2 nm), the more reactive sites when taking into account the solvent effect, are localized on the edges shared by a {111} and a {100} face in the case of the cuboctahedral and decahedral nanoparticles, and on the vertices in the case of the icosahedral nanoparticle. Our calculations also showed that the silver nanoparticles studied present a softer chemical behavior in water solution than in the gas phase. Comparison between the Ag nanoparticles reactivity and the Ag^+ reactivity gives us a better understanding of some experimental findings.[5] The radical character of the silver nanoparticles assumed in some works[3,5,6] as the origin of their biocide activity is in agreement with our findings. Further theoretical studies on the dependence of the Ag nanoparticles reactivity with respect to distinct parameters such as size, shape, and surface oxidation are in order.

Acknowledgments

M.T. Vázquez and O. Jiménez have provided the information requested. Part of this work was carried out on the computers of DGSCA, UNAM. R.E.E.S., H.B., and M.J.Y. would also like to thank the International Center for Nanotechnology and Advanced Materials (ICNAM) at UTSA.

Keywords: silver nanoparticles · surface reactivity · bactericidal properties · Fukui functions · molecular electrostatic potential · DFT studies

How to cite this article: R. E. Estrada-Salas, H. Barrón, A. A. Valladares, M. José-Yacamán, *Int. J. Quantum Chem.* **2012,** *112*, 3033–3038. DOI: 10.1002/qua.24207

[1] J. L. Elechiguerra, J. L. Burt, J. R. Morones, A. Camacho-Bragado, X. Gao, H. H. Lara, M. J. Yacaman, *J. Nanobiotechnol.* **2005**, *3, 6:* 1.
[2] L. A. Diaz-Torres, D. Ferrer, M. J. Yacaman, The Third San Antonio Biophotonics Symposium, San Antonio, TX. March 28–29, **2008**.
[3] J. R. Morones, J. L. Elechiguerra, A. Camacho, K. Holt, J. B. Kouri, J. Tapia Ramírez, M. J. Yacaman, *Nanotechnology* **2005**, *16,* 2346.
[4] M. Rai, A. Yadav, A. Gade, *Biotechnol. Adv.* **2009**, *27,* 76.
[5] B. Despax, C. Saulou, P. Raynaud, L. Datas, M. Mercier-Bonin, *Nanotechnology* **2011**, *22, 175101:* 1.
[6] J. S. Kim, E. Kuk, K. N. Yu, J. H. Kim, S. J. Park, H. J. Lee, S. H. Kim, Y. K. Park, Y. H. Park, C. Y. Hwang, Y. K. Kim, Y. S. Lee, D. H. Jeong, M. H. Cho, *Nanomedicine* **2007**, *3,* 95.
[7] C. N. Lok, C. M. Ho, R. Chen, Q. Y. He, W. Y. Yu, H. Sun, P. K. H. Tam, J. F. Chiu, C. M. Che, *J. Biol. Inorg. Chem.* **2007**, *12,* 527.
[8] S. Pal, Y. K. Tak, J. M. Song, *Appl. Environ. Microbiol.* **2007**, *73,* 1712.
[9] F. De Proft, J. M. L. Martin, P. Geerlings, *Chem. Phys. Lett.* **1996**, *256,* 400.
[10] R. Estrada-Salas, A. A. Valladares, *J. Mol. Struct. Theochem.* **2008**, *869,* 1.
[11] R. Estrada-Salas, A. A. Valladares, *J. Phys. Chem. A* **2009**, *113,* 10299.
[12] I. Levine, Quantum Chemistry, 5th ed.; Prentice Hall: New Jersey, **2000**.
[13] R. G. Parr, W. Yang, Density-Functional Theory of Atoms and Molecules; Oxford University Press: New York, **1989**.
[14] A. D. McNaught, A. Wilkinson, IUPAC Compendium of Chemical Terminology–The Gold Book; Blackwell Science: Cambridge, **1997**. http://goldbook.iupac.org. Accessed on June 21, 2012.
[15] R. G. Pearson, *Proc. Natl. Acad. Sci. USA* **1986**, *83,* 8440.
[16] B. Delley, *J. Chem. Phys.* **1990**, *92,* 508.
[17] B. Delley, *J. Chem. Phys.* **2000**, *113,* 7756.
[18] Materials Studio Release 4.4; Accelrys Software Inc.: San Diego, CA, USA, **2008**.
[19] B. Hammer, L. B. Hansen, J. K. Norskov, *Phys. Rev. B* **1999**, *59,* 7413.
[20] B. Delley, *J. Phys. Chem. A* **2006**, *110,* 13632.
[21] B. Delley, *Phys. Rev. B* **2002**, *66,155125:* 1.
[22] J. P. Perdew, J. A. Chevary, S. H. Vosko, K. A. Jackson, M. R. Pederson, D. J. Singh, C. Fiolhais, *Phys. Rev. B* **1992**, *46,* 6671.
[23] J. P. Perdew, K. Burke, M. Ernzerhof, *Phys. Rev. Lett.* **1996**, *77,* 3865.
[24] A. Klamt, G. Schüürmann, *J. Chem. Soc. Perkins Trans.* **1993**, *2,* 799.
[25] B. Delley, *Mol. Simul.* **2006**, *32,* 117.
[26] G. Schmid, *Chem. Soc. Rev.* **2008**, *37,* 1909.

Received: 29 February 2012
Revised: 29 February 2012
Accepted: 24 April 2012
Published online on 5 July 2012